

ISTITUTO NAZIONALE FISICA NUCLEARE

INFN/BE - 71/8

1 dicembre 1971

F. Demanins, G. Nardelli and G. Pauli

A MEASUREMENT OF THE ANGULAR DISTRIBUTIONS AND A DETERMINATION  
OF THE PHASE SHIFTS FOR THE ELASTIC SCATTERING OF NEUTRONS  
FROM  $^{12}\text{C}$  IN THE ENERGY RANGE 1.98 MeV TO 4.64 MeV.

A MEASUREMENT OF THE ANGULAR DISTRIBUTIONS AND A DETERMINATION  
OF THE PHASE SHIFTS FOR THE ELASTIC SCATTERING OF NEUTRONS FROM  
 $^{12}\text{C}$  IN THE ENERGY RANGE 1.98 MeV TO 4.64 MeV

F. Demanins

Istituto di Fisica, Università di Trieste

G. Nardelli

Istituto di Fisica, Università di Padova and Istituto Nazionale  
di Fisica Nucleare, Sezione di Padova

G. Pauli

Istituto di Fisica, Università di Trieste and Istituto Nazionale  
di Fisica Nucleare, Sezione di Trieste

A B S T R A C T

The elastic scattering of neutrons from carbon was studied in the incident neutron energy range 1.98 MeV to 4.64 MeV. Angular distributions were obtained by means of a neutron time-of-flight spectrometer. Data were taken for eight energies and for thirteen scattering angles. A phase-shift analysis was carried out and a set of phase angles was obtained capable of reproducing the elastic data. The phase shifts were used to calculate the scattered neutron polarization at different energies and angles, and the result was compared with the experimental data of various authors.

## 1. - INTRODUCTION

The elastic scattering of neutrons from  $^{12}\text{C}$  over the incident neutron energy range from about 2 MeV up to about 4.6 MeV has been the object of several measurements.

At the time the present work was undertaken, previous measurements concerning the angular distributions of the elastically scattered neutrons included the work of Wills, Bair, Cohn and Willard (<sup>1</sup>), Goldberg, May and Stehn (<sup>2</sup>), Gorlov, Lebedeva and Morozov (<sup>3</sup>), Lister and Sayres (<sup>4</sup>); the polarization of the scattered neutrons had been treated by McCormac, Steuer, Bond and Hereford (<sup>5</sup>), Elvin and Lane (<sup>6</sup>), Wenzel and Steuer (<sup>7</sup>), and Miller and Biggerstaff (<sup>8</sup>); the neutron total cross-section was that reported in the compilation of Stehn, Goldberg, Magurno and Wiener-Chasman (<sup>9</sup>).

In the energy range mentioned above, four resonances were observed in the  $^{12}\text{C}+n$  interaction at  $E_n = 2.076$  MeV ( $5/2^+$ ),  $E_n = 2.95$  MeV ( $3/2^+$ ),  $E_n = 3.60$  MeV ( $3/2^+$ ), and  $E_n = 4.25$  MeV ( $1/2^-$ ).  $E_n$  is the incident neutron energy at resonance, in the laboratory reference system.

In the present investigation the angular distributions of the neutrons elastically scattered from  $^{12}\text{C}$  were measured for eight incident neutron energies between 1.98 MeV and 4.64 MeV. Moreover, phase shifts were extracted from the experimental data using the total cross-section data of ref.(<sup>9</sup>). The phase-shift analysis was performed assuming as a starting set the phase angles reported in ref.(<sup>1</sup>) and ref.(<sup>4</sup>). The phase shifts thus derived were then used for calculating the polarization of the elastically scattered neutrons for various energies and angles. Finally, the predicted values of the polarization were compared with experimental data found in the literature, in order to check, in this way, the reliability of the set of phase angles previously determined.

## 2. - EXPERIMENTAL PROCEDURE

The experimental equipment used for carrying out the measurements described in this report consisted of a neutron time-of-flight spectrometer with pulsed beam.

Neutrons were produced by the reactions  $T(p,n)^3\text{He}$  and  $D(d,n)^3\text{He}$ . The ions accelerated by the 5.5 MeV Van de Graaff of the "Laboratori Nazionali dell'I.N.F.N." (Legnaro) were incident on targets of tritium or deuterium absorbed in titanium.

The carbon scattering sample was of cylindrical shape, having a diameter of 2.5 cm and a height of 4 cm. The sample was placed at a distance of 10 cm from the neutron source and with its axis perpendicular to the accelerator beam direction.

The angular distributions of the neutrons elastically scattered by the sample were measured using a neutron time-of-flight spectrometer with n- $\gamma$  discrimination. The spectrometer had two arms for the simultaneous and independent measurement of the time-of-flight of neutrons scattered at two different angles. The measurements were made with the spectrometer arms set along directions forming supplementary angles with respect to the axis of the incident neutron beam. The pulses of the two detectors were separately accepted by the two 256-channel subgroups of a 512-channel analyser. The normalization of the measurements was made using either a monitor situated at  $90^\circ$  to the accelerator beam and a charge integrator connected to the target.

The measurements reported hereinafter were made for 8 values of the incident neutron energy  $E_n$ , that is, 1.98, 2.24, 2.49, 2.74, 2.98, 3.20, 4.10 and 4.64 MeV; and for 13 values of the scattering angle  $\vartheta$  in the range from  $30^\circ$  to  $150^\circ$ .  $E_n$  is given in the laboratory reference system. The background subtraction was performed for each value of the energy  $E_n$  and for each angle  $\vartheta$ . The experimental data were also corrected for multiple scattering in the sample. The absolute scale for the differential cross-sections was obtained by normalizing the integrated angular distribution at  $E_n = 2.49$  MeV to the value of the total cross-section for the same energy found in the literature ( $^\circ$ ).

### 3. - PHASE-SHIFT ANALYSIS

The phase-shift analysis of the elastic scattering, which is the unique mode of scattering for the neutron energies under consideration, can be easily carried out since the target nucleus is a spin-0 nucleus.

One knows that the experimental data of the  $^{12}\text{C}(n,n)^{12}\text{C}$  differential cross-section can be analysed as a sum of Legendre polynomials  $P_L(\cos \vartheta)$  through the L-th order:

$$(1) \quad \sigma(\vartheta) = \sum_L B_L P_L(\cos \vartheta)$$

On the other hand, the differential cross-section for the elastic scattering of a neutron by a spin-0 nucleus, for the case of unpolarized neutrons, is given by (10)

$$(2) \quad \sigma(\vartheta) = \frac{1}{K^2} \sum_L A_L P_L(\cos \vartheta)$$

In eq.(2), K denotes the wave number in the center-of-mass reference system and the coefficients  $A_L$  have the following expression:

$$(3) \quad A_L = \sum_{J_1} \sum_{J_2} \sum_{\ell_1=J_1-1/2}^{J_1+1/2} \sum_{\ell_2=J_2-1/2}^{J_2+1/2} Z^2(\ell_1 J_1 \ell_2 J_2; 1/2 L) \times \\ \times \sin \delta(\ell_1; J_1) \sin \delta(\ell_2; J_2) \cos[\delta(\ell_1; J_1) - \delta(\ell_2; J_2)]$$

where:  $\delta(\ell_i; J_i)$  denotes the phase shift corresponding to the orbital angular momentum  $\ell_i$  and to the total angular momentum  $J_i$ ;

$$Z(\ell_1 J_1 \ell_2 J_2; 1/2 L) = i^{L-\ell_1+\ell_2} [\hat{\ell}_1 \hat{\ell}_2 \hat{J}_1 \hat{J}_2 W(\ell_1 J_1 \ell_2 J_2; 1/2 L) \langle L0 | \ell_1 \ell_2 00 \rangle$$

$$\text{where } \hat{a} = (2a+1)^{1/2};$$

$W(abcde; fg)$  are the Racah coefficients;

$\langle ab | cdef \rangle$  are the Clebsch-Gordan coefficients.

The relationship between the coefficients  $B_L$  of Eq.(1), which are derived by fitting the experimental data, and the coefficient  $A_L$  of Eq.(2), which are related to the phase shifts through Eq.(3), is:

$$B_L = \frac{1}{K^2} A_L = \frac{1}{K^2} \sum_{J_1 J_2 \ell_1 \ell_2} Z^2(\ell_1 J_1 \ell_2 J_2; 1/2 L) \sin \delta(\ell_1; J_1) \times \\ \times \sin \delta(\ell_2; J_2) \cos [\delta(\ell_1; J_1) - \delta(\ell_2; J_2)]$$

The analysis of the experimental data by means of the sum (1) was carried out up to  $L_{\max} = 4$ . Higher values of  $L$  did not improve the fit of the experimental data. This means that  $f$  waves need not be included in the phase-shift analysis in order to reproduce the experimental data.

Using Eq. (3) for  $0 \leq L \leq 4$ , the following expressions for the coefficients  $A_L$  are obtained:

$$A_0 = D(0\frac{1}{2}; 0\frac{1}{2}) + D(1\frac{1}{2}; 1\frac{1}{2}) + 2D(1\frac{3}{2}; 1\frac{3}{2}) + 2D(2\frac{3}{2}; 2\frac{3}{2}) + 3D(2\frac{5}{2}; 2\frac{5}{2})$$

$$A_1 = 2D(0\frac{1}{2}; 1\frac{1}{2}) + 4D(0\frac{1}{2}; 1\frac{3}{2}) + 4D(1\frac{1}{2}; 2\frac{3}{2}) + \frac{4}{5}[D(1\frac{3}{2}; 2\frac{3}{2}) + 9D(1\frac{3}{2}; 2\frac{5}{2})]$$

$$A_2 = 4D(0\frac{1}{2}; 2\frac{3}{2}) + 6D(0\frac{1}{2}; 2\frac{5}{2}) + 4D(1\frac{1}{2}; 1\frac{3}{2}) + 2D(1\frac{3}{2}; 1\frac{3}{2}) + 2D(2\frac{3}{2}; 2\frac{3}{2}) + \frac{4}{7}[D(2\frac{3}{2}; 2\frac{5}{2}) + 2D(2\frac{5}{2}; 2\frac{5}{2})]$$

$$A_3 = 6D(1\frac{1}{2}; 2\frac{5}{2}) + \frac{12}{5}[3D(1\frac{3}{2}; 2\frac{3}{2}) + 2D(1\frac{3}{2}; 2\frac{5}{2})]$$

$$A_4 = \frac{18}{7}[4D(2\frac{3}{2}; 2\frac{5}{2}) + D(2\frac{5}{2}; 2\frac{5}{2})]$$

where

$$D(\ell_1, J_1; \ell_2, J_2) = \sin \delta(\ell_1; J_1) \sin \delta(\ell_2; J_2) \cos [\delta(\ell_1; J_1) - \delta(\ell_2; J_2)]$$

One may now derive the five phase angles from the measured angular distributions and from the total cross-section data, using the preceding expressions for the  $A_L$ . The analysis must be carried out taking into account the following requirements:

- a) the phase shifts are continuous functions of the energy,
- b) over a resonance there must be no unusual variation of too many phase-shifts,

c) over a resonance one phase shift must increase by about  $180^\circ$  with increasing energy. Moreover, it must be noticed <sup>(11)</sup> that  $\cos \delta(\ell_i; J_i)$  is a symmetric function and  $\sin \delta(\ell_i; J_i)$  is an antisymmetric function and therefore the cross-section is invariant with respect to a change of the sign of all the phase angles. The cross-section is also invariant if the phase angles  $\delta(\ell; \ell + \frac{1}{2})$  are interchanged with the phase angles  $\delta(\ell; \ell - \frac{1}{2})$  for all values of  $\ell$ .

The independent set of phase shifts which is obtained with the preceding analysis, can now be put in relation to the polarization of neutrons in the scattering process. In fact, the scattering of polarised neutrons by a spin-0 nucleus is described by a cross-section having the following expression (<sup>2</sup>):

$$\sigma_P(\vartheta) = \frac{1}{K^2} \sum_L C_L P'_L(\cos \vartheta)$$

where

$$P'_L(\cos \vartheta) = \sin \vartheta \frac{d P_L(\cos \vartheta)}{d(\cos \vartheta)}$$

Now, the coefficients  $C_L$  are related to the phase angles  $\delta(\ell_i; J_j)$  which appear in Eq.(2) through the relation

$$C_L = \left[ \frac{3(2L+1)}{2L(L+1)} \right]^{1/2} \sum_{J_1 J_2 \ell_1 \ell_2} (-)^{J_1 + \ell_2 - L + 1/2} Z^2(\ell_1 J_1 \ell_2 J_2; 1/2 L) \times \\ \times \frac{X(J_1 \ell_1 1/2; J_2 \ell_2 1/2; L L 1)}{W(\ell_1 J_1 \ell_2 J_2; 1/2 L)} \sin \delta(\ell_1; J_1) \sin \delta(\ell_2; J_2) \sin[\delta(\ell_1; J_1) - \delta(\ell_2; J_2)]$$

where

$$X(J_1 \ell_1 1/2; J_2 \ell_2 1/2; L L 1) = (-)^S \sum_z [z^2 W(\ell_1 J_2 1/2 L; z J_1) \times \\ \times W(J_2 \ell_1 1/2 L; z \ell_2) W(L 1/2 L 1/2; z 1)]$$

where

$$S = J_1 + J_2 + \ell_1 + \ell_2 + 2(L+1)$$

Then, the expressions of the coefficients  $C_L$  for  $0 \leq L \leq 4$  are the following:

$$C_1 = -2P(0 1/2; 1 1/2) + 2P(0 1/2; 1 3/2) - 2P(1 1/2; 2 3/2) - \\ - \frac{2}{5} [4P(1 3/2; 2 3/2) - 9(1 3/2; 2 5/2)]$$

$$C_2 = -2P(0 1/2; 2 3/2) + 2P(0 1/2; 2 5/2) + 2P(1 1/2; 1 3/2) + \\ + \frac{10}{7} P(2 3/2; 2 5/2)$$

$$C_3 = 2P(1\frac{1}{2}; 2\frac{5}{2}) - \frac{2}{5}[6P(1\frac{3}{2}; 2\frac{3}{2}) - P(1\frac{3}{2}; 2\frac{5}{2})]$$

$$C_4 = \frac{18}{7}P(2\frac{3}{2}; 2\frac{5}{2})$$

where

$$P(\ell_1 J_1; \ell_2 J_2) = \sin\delta(\ell_1; J_1)\sin\delta(\ell_2; J_2)\sin[\delta(\ell_1; J_1) - \delta(\ell_2; J_2)].$$

#### 4. - RESULTS

In Figures 1 and 2 are plotted the angular distributions of the neutrons elastically scattered by  $^{12}\text{C}$  which were measured at the eight values of the incident neutron energy  $E_n$ , from 1.98 MeV to 4.64 MeV, specified in section 2. The scattering angles are referred to the center of mass. The solid-line curves represent the result of the phase-shift analysis.

The values of the phase-shifts are listed in Table I together with the energies at which they were determined. The behaviour of the phase shifts as a function of the neutron energy is displayed in Fig. 3.

The phase shifts were obtained using the relationships of the preceding section and fitting the angular distributions measured at the above-mentioned incident neutron energies (closed symbols). Intermediate values (open symbols) were determined taking into account the behaviour of the total cross-section as a function of the neutron energy. The continuous lines are drawn as a visual aid through the calculated points. For the first stage of the analysis, the sets of phase-shifts given by Wills, Bair, Cohn and Willard (<sup>1</sup>) and Lister and Sayres (<sup>4</sup>) were used.

In the energy range covered by the present analysis, the phase  $s\frac{1}{2}$  and  $p\frac{3}{2}$  appear to vary weakly. The variation of the phase  $d\frac{5}{2}$  around 2.076 MeV is associated with the resonance at that energy. Similarly, the variations of the phase  $d\frac{3}{2}$  are associated with the resonances at 2.95 MeV and 3.67 MeV, and the phase  $p\frac{1}{2}$  is associated with the resonance at 4.25 MeV.

A resonance at 2.815 MeV was observed by Cierjaks et al. (<sup>13</sup>) in a measurement of the neutron total cross-section. No other data for neu-

trons concerning this resonance could be found in the literature. Lack of sufficient information prevented the determination of the parameters characterizing this resonance and therefore the corresponding energy interval was left blank in the figures.

The coefficients  $B_L$  as a function of  $E_n$ , which were obtained from the analysis, are reported in Figs. 4, 5, 6, 7 and 8. The data of the present work are denoted by the triangles, the closed and open triangles having the meaning already states in connection with Fig. 3. Such data are compared with those deduced from the measurements described in ref. (1), (4), (14). The values of the coefficients  $B_L$  are listed in Table II together with the energies at which they were determined.

The reliability of the phase shifts obtained in the present work can be checked by comparing with experimental data found in the literature the neutron polarization which can be calculated with the formula

$$(4) \quad P(\vartheta, E) = \frac{\sigma_p(\vartheta, E)}{\sigma(\vartheta, E)} = \frac{\sum_L C_L(E) P'_L(\cos \vartheta)}{\sum_L A_L(E) P_L(\cos \vartheta)}$$

using the coefficients  $C_L$  given in the preceding section. In Fig. 9 the predicted polarization (continuous curve) is compared with the data of McCormac et al. (5) for  $E_n = 3.1$  MeV; in Fig. 10 comparison is made with the data of Elwin and Lane (6) and Purser et al. (15) for  $E_n = 2.4$  MeV, and with the data of Gorlov et al. (3) for  $E_n = 4.0$  MeV and in Fig. 11 with the data of Kelsey et al. (16) for  $E_n = 4.4$  MeV. In Fig. 12 the predicted polarization for neutrons scattered through  $48^\circ 23'$  and  $94^\circ 48'$  in the energy range from 2 MeV to 2.5 MeV, represented by the triangles connected by the continuous curve, is compared with the polarization measured by Elwin and Lane (6). In Fig. 13 a similar comparison for neutrons scattered through  $135^\circ$  and in the energy range from 2.5 MeV to 4.5 MeV, using the data of Wenzel and Steuer (7), Miller and Biggerstaff (8) and Gorlov et al. (3), is shown.

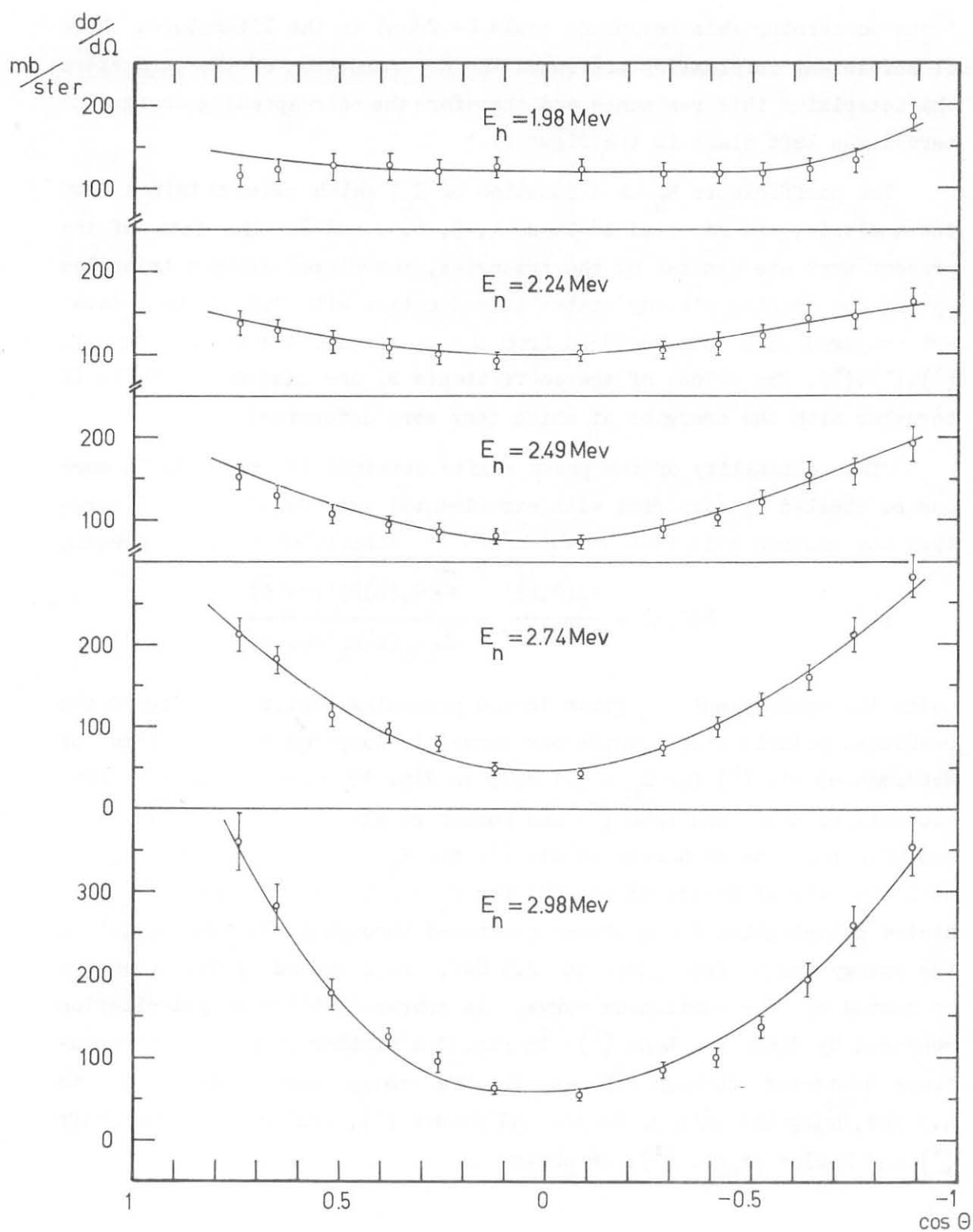


Fig. 1 - Center-of-mass differential cross-sections for  $^{12}\text{C}(n,n)^{12}\text{C}$  for incident neutron energies of 1.98, 2.24, 2.49, 2.74 and 2.98 MeV. The solid curves were calculated from the phase shifts of Table I and Fig. 3.

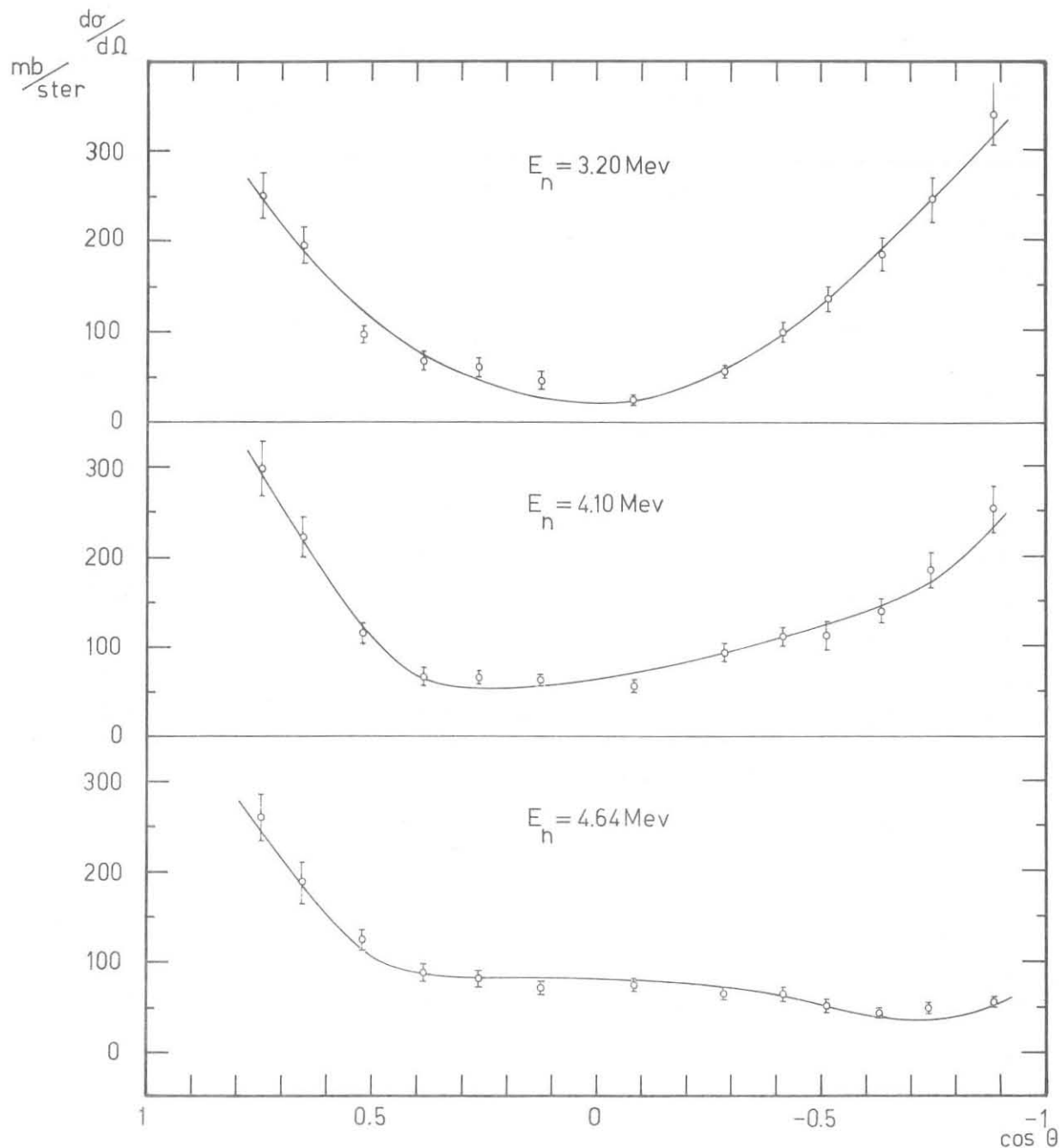


Fig. 2 - Center-of-mass differential cross-sections for  $^{12}\text{C}(n,n)^{12}\text{C}$  for incident neutron energies of 3.20, 4.10 and 4.64 MeV. The solid curves were calculated from the phase shifts of Table I and Figure 3.

TABLE I - Phase shifts for  $^{12}\text{C}(n,n)^{12}\text{C}$ .

$E_n$ (MeV)	$\delta(0, \frac{1}{2})$	$\delta(1, \frac{1}{2})$	$\delta(1, \frac{3}{2})$	$\delta(2, \frac{3}{2})$	$\delta(2, \frac{5}{2})$
1,98	-91° 27'	-5° 36'	-2° 54'	9° 20'	3° 50'
2,00	-91° 36'	-5° 39'	-2° 56'	9° 32'	4°
2,05	-92° 6'	-5° 45'	-2° 58'	10° 5'	5° 30'
2,08	-92° 21'	-5° 46'	-3°	10° 24'	170°
2,10	-92° 36'	-5° 48'	-3°	10° 43'	173°
2,15	-93° 12'	-5° 51'	-3° 2'	11° 28'	175° 30'
2,20	-94° 43'	-5° 56'	-3° 5'	12° 21'	176° 15'
2,24	-94° 9'	-6° 6'	-3° 6'	13°	176° 30'
2,40	-96° 24'	-6° 14'	-3° 13'	17° 3'	177° 25'
2,49	-97° 42'	-6° 25'	-3° 24'	20°	177° 48'
2,74	-101° 42'	-6° 54'	-3° 30'	30°	178°
2,80	-102° 40'	-7° 3'	-3° 30'	38° 30'	178°
2,85	-103° 24'	-7° 12'	-3° 33'	50°	178°
2,90	-104° 8'	-7° 19'	-3° 36'	68° 30'	178°
2,95	-104° 50'	-7° 30'	-3° 36'	95°	178°
2,98	-105° 12'	-7° 36'	-3° 36'	127°	178°
3,00	-105° 30'	-7° 36'	-3° 39'	158°	177° 50'
3,05	-106° 6'	-7° 45'	-3° 42'	190°	177° 40'
3,10	-106° 36'	-7° 55'	-3° 48'	203°	177° 24'
3,20	-107° 24'	-8° 18'	-3° 54'	221°	176°
3,40	-109° 12'	-9° 8'	-4° 48'	224° 30'	175° 28'
3,60	-110° 12'	-9° 56'	-6° 26'	262°	174° 36'
3,80	-111° 18'	-10° 45'	-8° 24'	282°	173° 55'
4,00	-117° 35'	-11° 35'	-10° 44'	298°	173° 15'
4,10	-118°	-12°	-12°	300°	173°
4,20	-118° 15'	-36°	-12°	305° 30'	172° 36'
4,25	-116° 24'	121° 43'	-11° 45'	308°	172° 27'
4,30	-117° 18'	111° 58'	-11° 23'	310° 40'	172° 17'
4,40	-115° 12'	124° 8'	-10° 29'	315° 45'	171° 57'
4,50	-112° 24'	132° 20'	-9° 25'	321°	171° 36'
4,64	-108°	140°	-8°	328°	171°

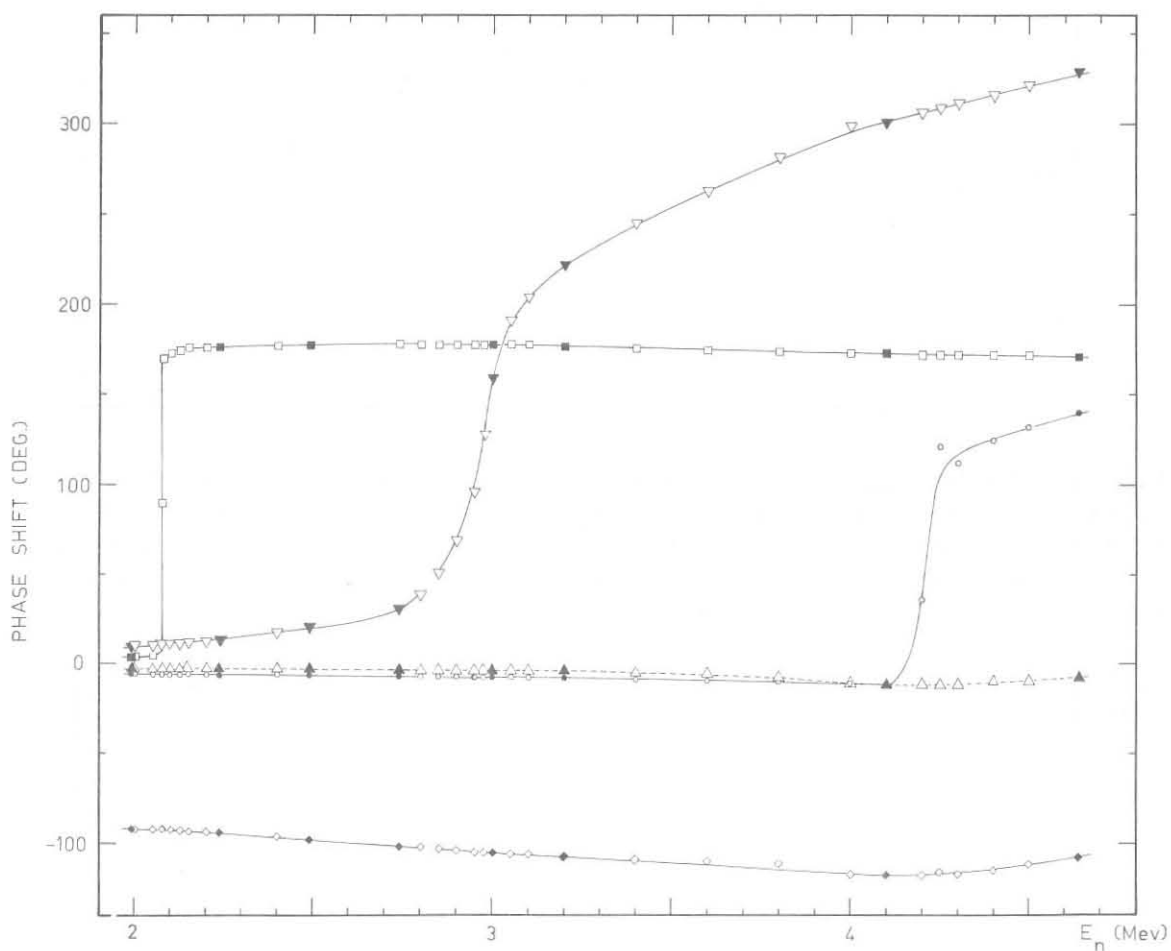


Fig. 3 - The phase shifts for  $^{12}\text{C}(n,n)^{12}\text{C}$  plotted as a function of neutron energy (Lab):  $\diamond \blacklozenge \delta(0; \frac{1}{2})$ ,  $\circ \bullet \delta(1; \frac{1}{2})$ ,  $\triangle \blacktriangle \delta(1; \frac{3}{2})$ ,  $\nabla \blacktriangledown \delta(2; \frac{3}{2})$ ,  $\square \blacksquare \delta(2; \frac{5}{2})$ . In this figure and in the following ones the energy interval from 2.8 MeV to 2.83 MeV has been left blank for the reasons explained in the text.

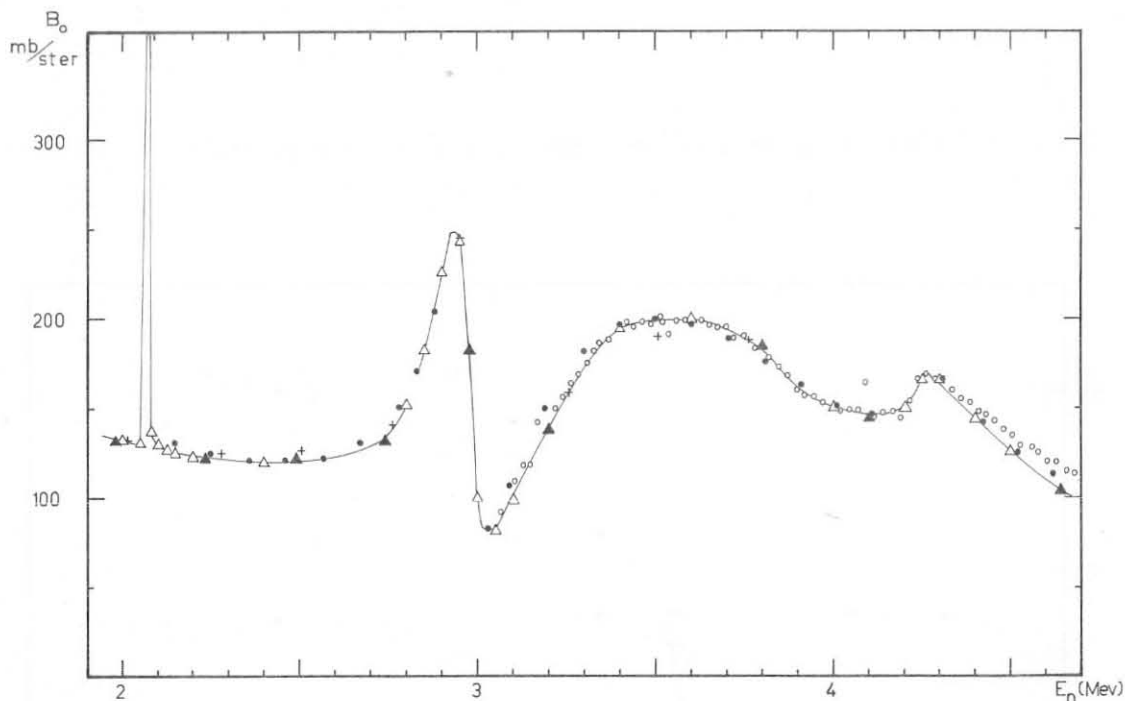


Fig. 4 - The Legendre coefficient  $B_0$  for  $^{12}\text{C}(n,n)^{12}\text{C}$  plotted as a function of neutron energy (Lab). The curve was calculated from the phase shifts of Table I. Comparison with the results of Wills et al. (ref.(1)), Lister and Sayres (ref.(4)) and Metellini (ref.(14)) is shown.  $\Delta$   $\blacktriangle$  this work,  $+$  ref.(1),  $\circ$  ref.(4),  $\bullet$  ref.(14).

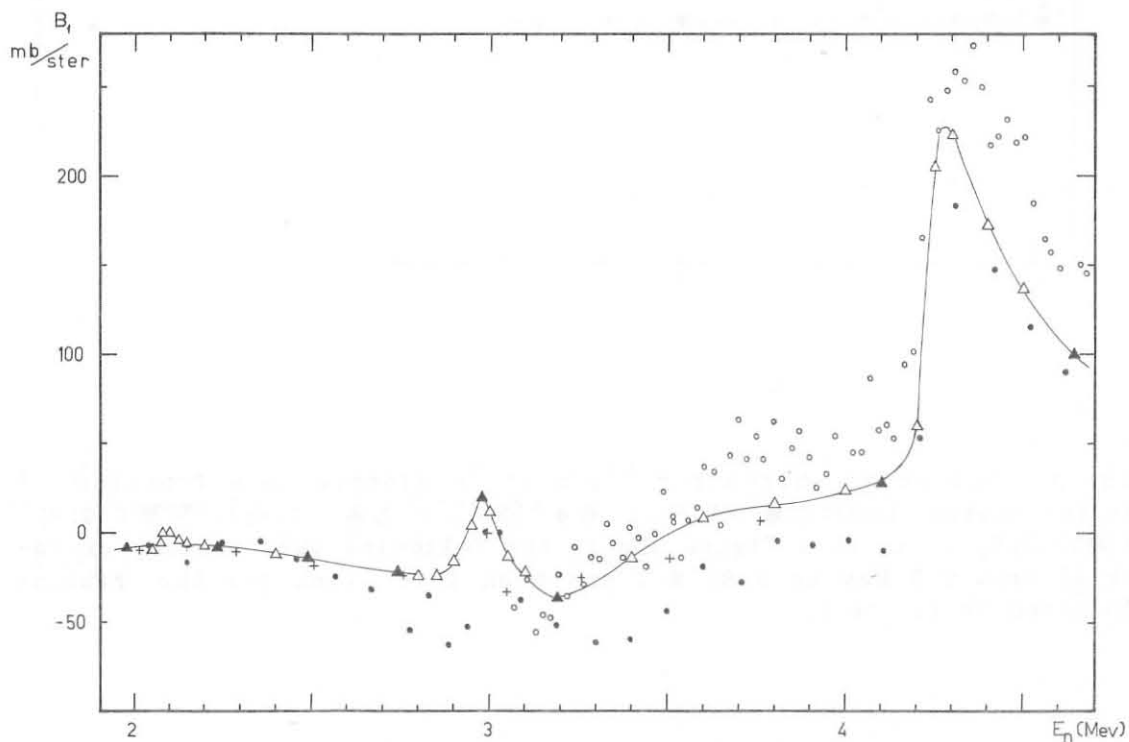


Fig. 5 - The Legendre coefficient  $B_1$  for  $^{12}\text{C}(n,n)^{12}\text{C}$  plotted as a function of neutron energy (Lab). The curve was calculated from the phase shifts of Table I. Comparison with the results of Wills et al. (ref.(1)), Lister and Sayres (ref.(4)) and Metellini (ref.(14)) is shown.  $\Delta$   $\blacktriangle$  this work,  $+$  ref.(1),  $\circ$  ref.(4),  $\bullet$  ref.(14).

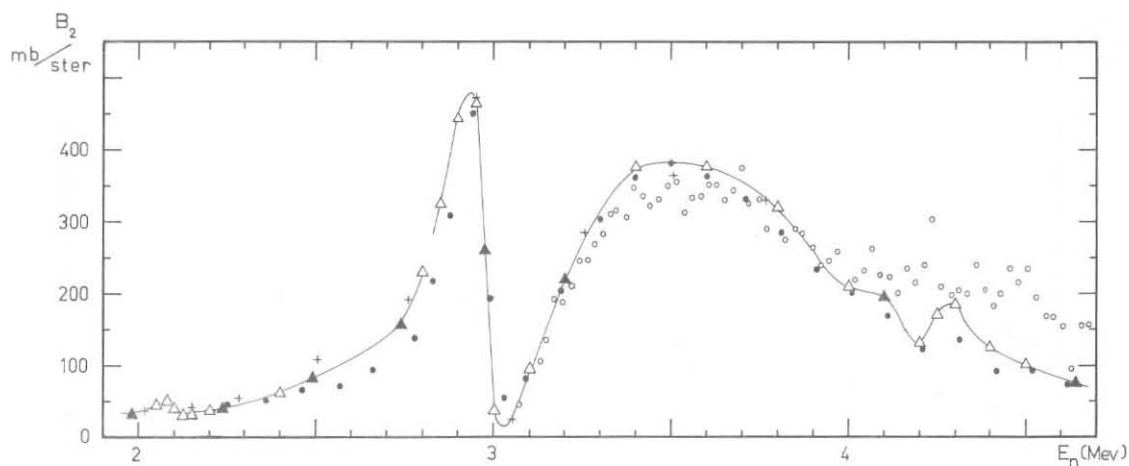


Fig. 6 - The Legendre coefficient  $B_2$  for  $^{12}\text{C}(n,n)^{12}\text{C}$  plotted as a function of neutron energy (Lab). The curve was calculated from the phase shifts of Table I. Comparison with the results of Wills et al. (ref.(1)), Lister and Sayres (ref.(4)) and Metellini (ref.(14)) is shown.  $\Delta$   $\blacktriangle$  this work,  $+$  ref.(1),  $\circ$  ref.(4),  $\bullet$  ref.(14).

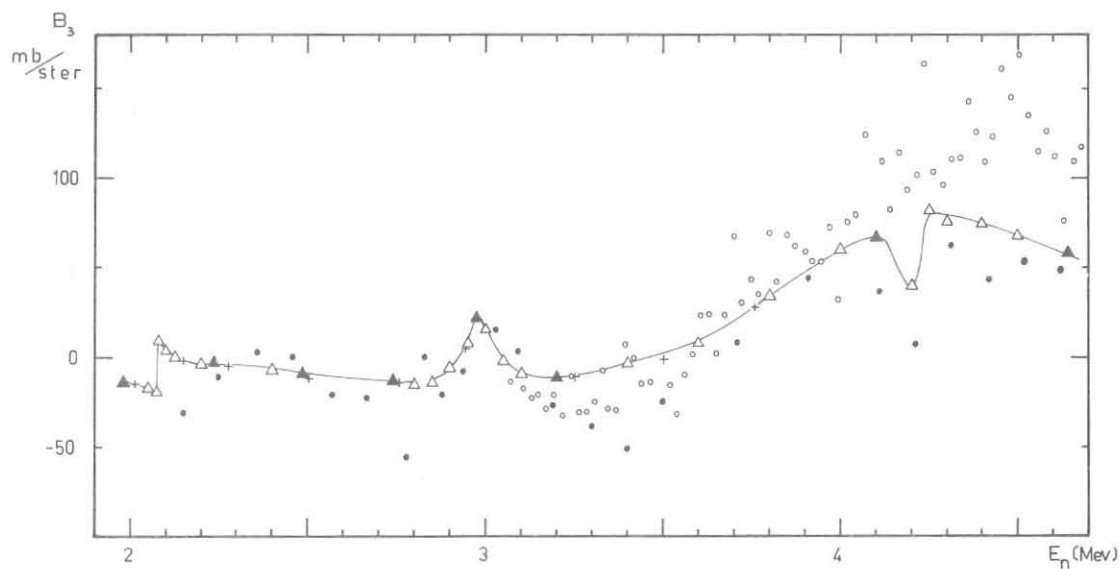


Fig. 7 - The Legendre coefficient  $B_3$  for  $^{12}\text{C}(n,n)^{12}\text{C}$  plotted as a function of neutron energy (Lab). The curve was calculated from the phase shifts of Table I. Comparison with the results of Wills et al. (ref.(1)), Lister and Sayres (ref.(4)) and Metellini (ref.(14)) is shown.  $\Delta$   $\blacktriangle$  this work,  $+$  ref.(1),  $\circ$  ref.(4),  $\bullet$  ref.(14).

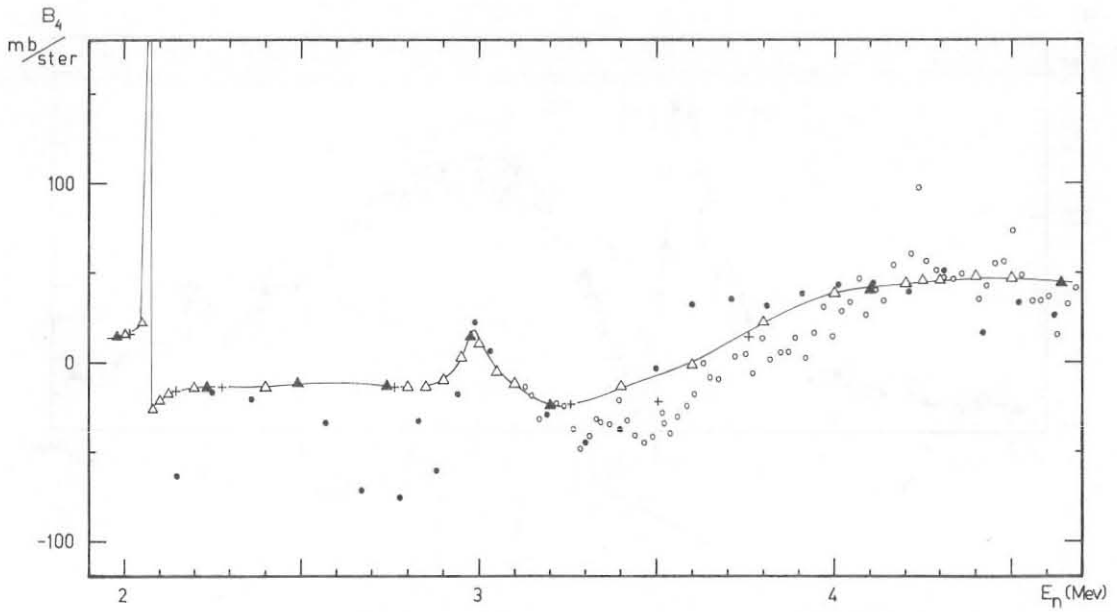


Fig. 8 - The Legendre coefficient  $B_4$  for  $^{12}\text{C}(n,n)^{12}\text{C}$  plotted as a function of neutron energy (Lab). The curve was calculated from the phase shifts of Table I. Comparison with the results of Wills et al. (ref. (1)), Lister and Sayres (ref. (4)) and Metellini (ref. (14)) is shown.  $\Delta$   $\blacktriangle$  this work,  $+$  ref. (1),  $\circ$  ref. (4),  $\bullet$  ref. (14).

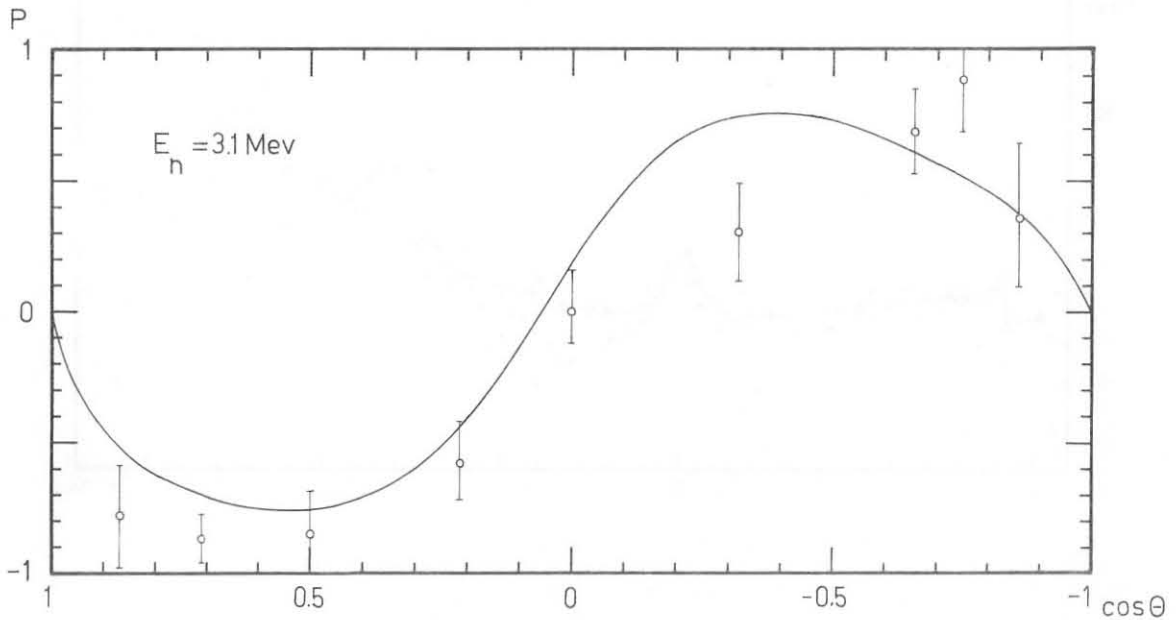


Fig. 9 - Calculated curve of the polarization of neutrons scattered elastically by  $^{12}\text{C}$  as a function of the center-of-mass scattering angle for  $E_n = 3.1$  Mev. Comparison with the experimental data of McCormac et al. (5) is shown.

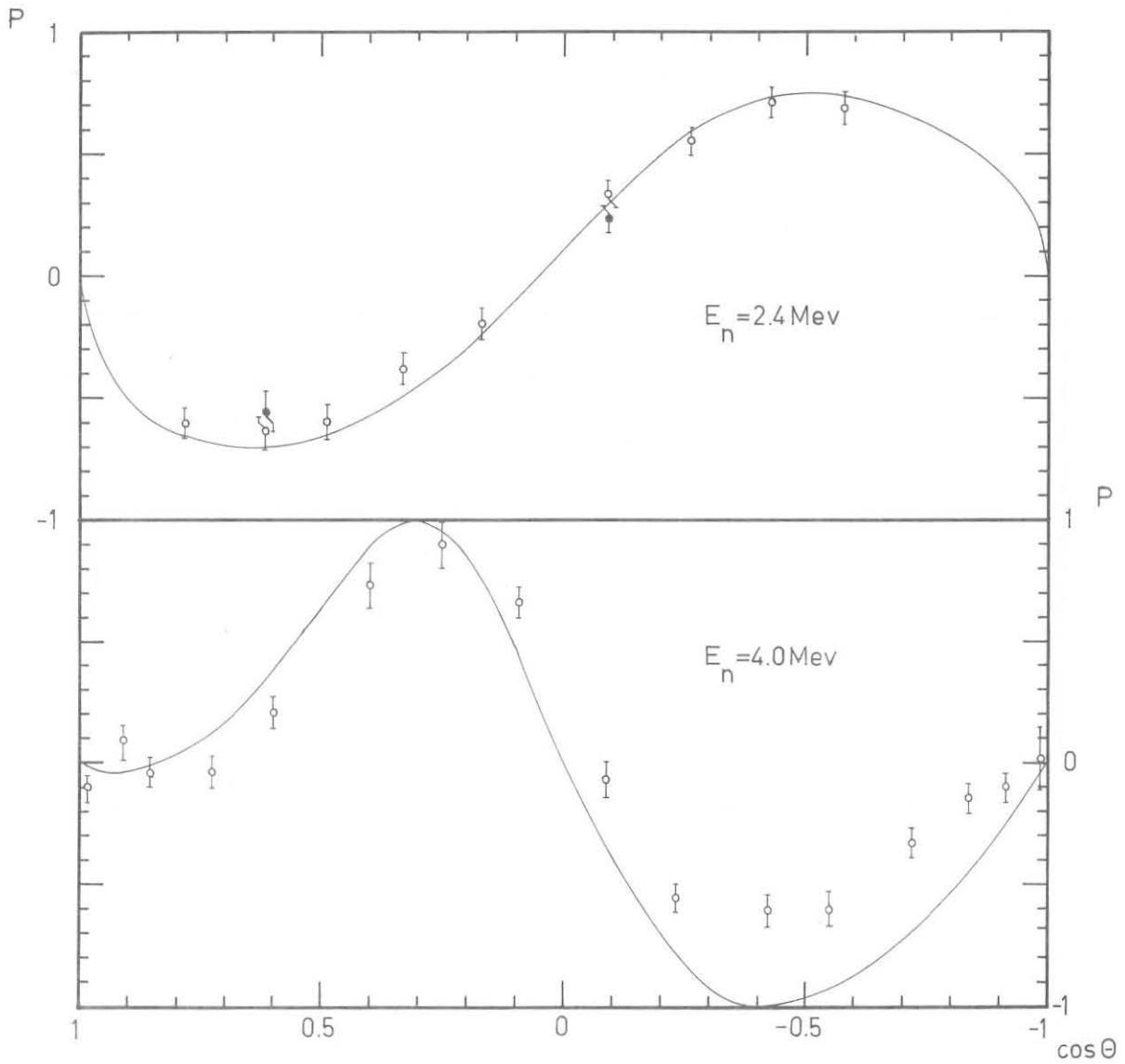


Fig. 10 - Calculated curves of the polarization of neutrons scattered elastically by  $^{12}\text{C}$  as a function of the center-of-mass scattering angle for  $E_n = 2.4 \text{ MeV}$  and  $E_n = 4.0 \text{ MeV}$ . Comparison with the experimental data for  $E_n = 2.4 \text{ MeV}$  reported by Purser et al. ( $\circ$ ) (ref. (15)) and Elwin and Lane ( $\bullet$ ) (ref. (6)), and with the experimental data for  $E_n = 4.0 \text{ MeV}$  reported by Gorlov et al. (ref. (3)) is shown.

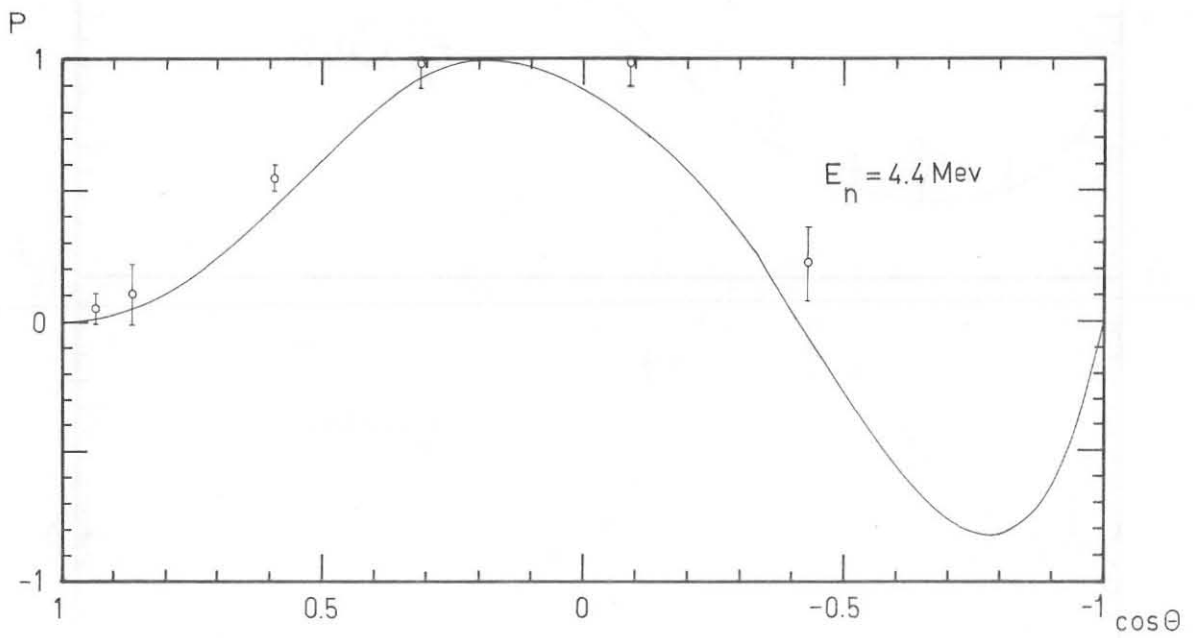


Fig. 11 - Calculated curve of the polarization of neutrons scattered elastically by  $^{12}\text{C}$  as a function of the center-of-mass scattering angle for  $E_n = 4.4 \text{ MeV}$ . Comparison with the experimental data of Kelsey et al. (ref. (16)) is shown.

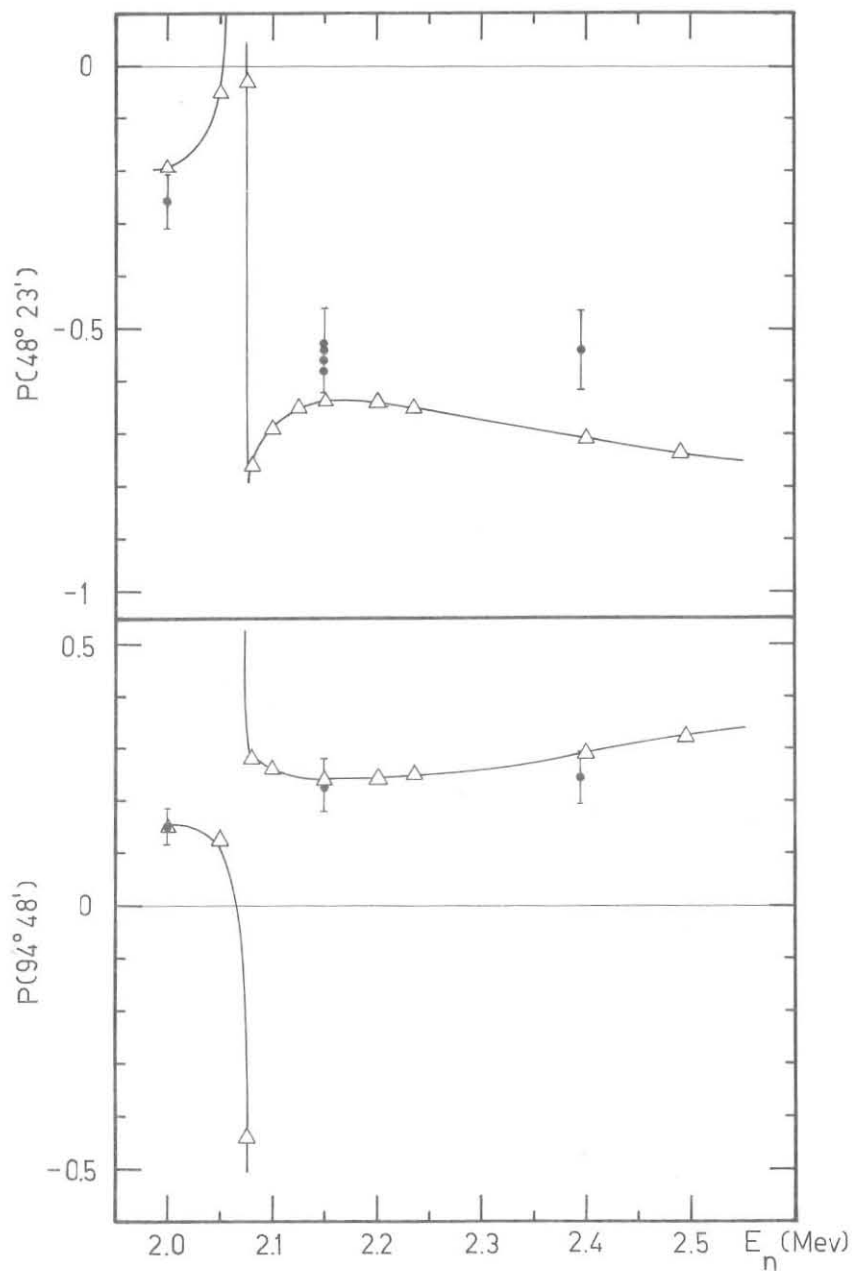


Fig- 12 - Calculated values, by means of Eq. (4), of the polarization of neutrons scattered elastically by  $^{12}\text{C}$  for center-of-mass angles  $48^\circ 23'$  and  $94^\circ 48'$  ( $\Delta$  and solid curve). Comparison with the experimental data of Elwin and Lane (ref. (6)) is shown.

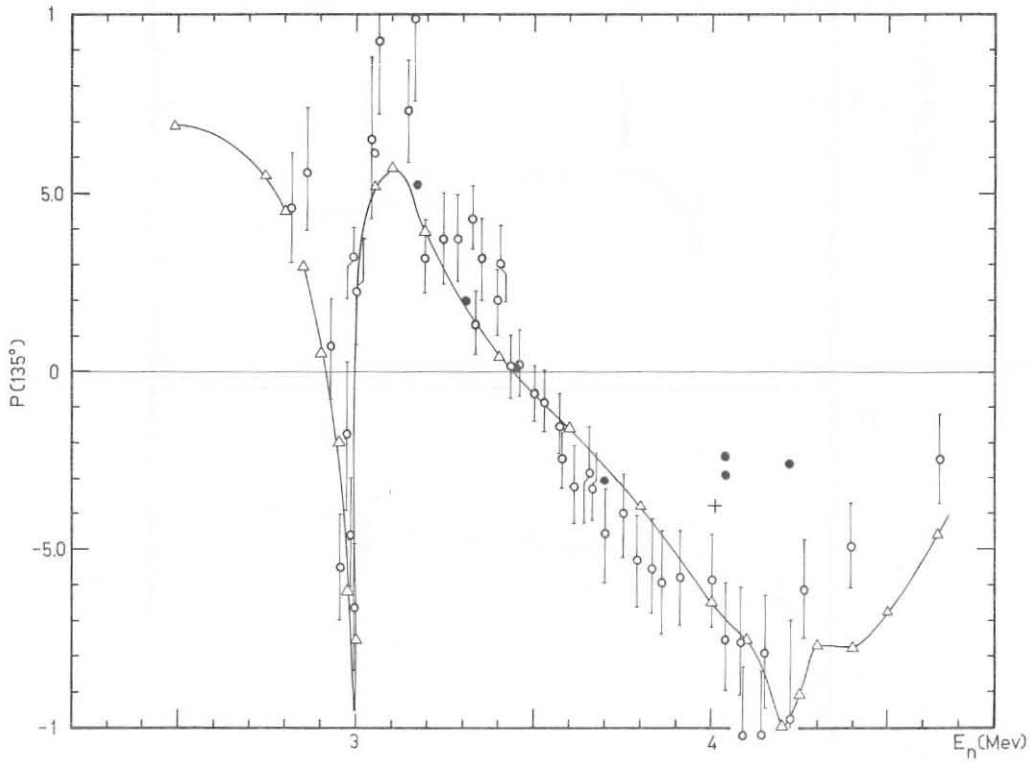


Fig. 13 - Calculated values, by means of Eq. (4), of the polarization of neutrons scattered elastically by  $^{12}\text{C}$  for the center-of-mass angle  $135^\circ$  ( $\Delta$  and solid curve). Comparison with the experimental data of Miller and Biggerstaff ( $\bullet$ ) (ref.(<sup>6</sup>)), of Gorlov et al. ( $+$ ) (ref.(<sup>3</sup>)) and Wenzel and Steuer ( $\circ$ ) (ref.(<sup>7</sup>)) is shown.

TABLE II - Legendre coefficients for  $^{12}\text{C}(n,n)^{12}\text{C}$ .

$E_n$ (MeV)	$B_L$ (mb/sr)				
	$B_0$	$B_1$	$B_2$	$B_3$	$B_4$
1,98	133	-9	33	-14	15
2,00	132	-9	56	-14	16
2,05	131	-11	44	-17	23
2,08	137	0	52	10	-26
2,10	131	-2	39	4	-21
2,15	126	-5	35	-1	-16
2,20	124	-7	38	-3	-14
2,24	122	-8	41	-3	-14
2,40	120	-12	63	-7	-14
2,49	121	-15	84	-9	-12
2,74	132	-22	158	-13	-13
2,80	152	-25	230	-15	-15
2,85	183	-24	326	-14	-14
2,90	227	-16	444	-8	-9
2,95	244	4	466	8	3
2,98	183	21	261	22	15
3,00	101	12	38	17	11
3,05	81	-14	27	-3	-5
3,10	99	-22	95	-9	-12
3,20	138	-26	222	-11	-24
3,40	195	13	378	-3	-13
3,60	198	9	378	9	-1
3,80	185	16	323	35	23
4,00	152	24	211	60	39
4,10	146	27	196	68	41
4,20	150	60	134	40	45
4,25	166	205	171	82	46
4,30	166	224	187	76	47
4,40	144	173	125	74	47
4,50	125	137	103	68	47
4,64	104	101	77	58	44

## 5. - CONCLUSION

The phase-shift analysis as described in the present work is capable of reproducing satisfactorily, in the energy range from 1.98 MeV to 4.64 MeV, (a) the experimental angular distributions of the neutrons elastically scattered by  $^{12}\text{C}$ , (b) the behaviour and the absolute value of the total cross-section (this is obtained by multiplying by  $4\pi$  the values of the coefficients  $B_0$  listed in Table II or the values represented by the points reported in Fig. 4), and (c) the data regarding the polarization.

There are discrepancies, such as that concerning the polarization at 4 MeV (Fig. 10) and that appearing in Fig. 13 for energies greater than 4.2 MeV, where the polarization was measured with an energy spread of  $320 \div 540$  keV. To shed light on this, further experimental information would be necessary.

Finally, it would be worthwhile to investigate the  $^{12}\text{C}(n,n)^{12}\text{C}$  reaction with the aim of ascertaining the presence of resonances between 2.8 MeV and 2.83 MeV and assigning the level parameters (spin and parity) of the  $^{13}\text{C}$  states which can be associated with them.

REFERENCES

- (<sup>1</sup>) J.E. Wills, J.K. Bair, H.O. Cohn and H.B. Willard: Phys. Rev. 109 (1958) 891.
- (<sup>2</sup>) M.D. Goldberg, V.M. May and J.R. Stehn: Brookhaven National Laboratory Report BNL-400, 2nd ed. (Office of Technical Services, Department of Commerce, Washington, D.C., 1963), Vol. 1.
- (<sup>3</sup>) G.V. Gorlov, N.S. Lebedeva and V.M. Morozov: Dokl. Akad. Nauk. SSSR 3 (1964) 574. (English Transl. Soviet Phys. Doklady 9 (1965) 806).
- (<sup>4</sup>) D. Lister and A. Sayres: Phys. Rev. 143 (1966) 745.
- (<sup>5</sup>) B.M. McCormac, M.F. Steuer, C.D. Bond and F.L. Hereford: Phys. Rev. 108 (1957) 116.
- (<sup>6</sup>) A.J. Elwin and R.O. Lane: Nucl. Phys. 31 (1962) 78.
- (<sup>7</sup>) B.E. Wenzel and M.F. Steuer: Phys. Rev. 137 (1965) B80.
- (<sup>8</sup>) T.G. Miller, J.A. Biggerstaff: Nucl. Phys. A124 (1969) 637.
- (<sup>9</sup>) J.R. Stehn, M.D. Goldberg, B.A. Magurno and R. Wiener-Chasman: Neutron Cross Sections, Brookhaven National Laboratory Report BNL-325, 2nd ed., Suppl. N. 2 (Office of Technical Services, Department of Commerce, Washington, D.C., 1964), Vol. 1.
- (<sup>10</sup>) J.M. Blatt and L.C. Biedenharn: Rev. Mod. Phys. 24 (1952) 258.
- (<sup>11</sup>) G. Pisent: Helv. Phys. Acta 36 (1963) 248.
- (<sup>12</sup>) A. Simon and T.A. Welton: Phys. Rev. 90 (1953) 1036.
- (<sup>13</sup>) S. Cierjaks, P. Forti, D. Kopsch, L. Kropp, J. Nebe and H. Unseld: Kernforschungszentrum Karlsruhe Report, KFK 1000/EUR 3963e/EANDC(E)-111"U" (June 1968).

- (<sup>14</sup>) A. Metellini : thesis, University of Padua (1970) unpublished.
- (<sup>15</sup>) F.O. Purser, J.R. Sawers, W.D. Andress, G.L. Morgan and R.L. Walter: AEC Washington Report, WASH-1048 (1964), p. 33, (unpublished)
- (<sup>16</sup>) C.A. Kelsey, S. Kobayashi and A.S. Mahajan: Nucl. Phys. 68 (1965) 413.

\* \* \*